Realization of compact tractor beams using acoustic delay-lines

A. Marzo, A. Ghobrial, L. Cox, M. Caleap, A. Croxford, and B. W. Drinkwater

Citation: Appl. Phys. Lett. **110**, 014102 (2017); doi: 10.1063/1.4972407
View online: http://dx.doi.org/10.1063/1.4972407
View Table of Contents: http://aip.scitation.org/toc/apl/110/1
Published by the American Institute of Physics

Realization of compact tractor beams using acoustic delay-lines

A. Marzo,[a] A. Ghobrial, L. Cox, M. Caleap, A. Croxford, and B. W. Drinkwater
Faculty of Engineering, University of Bristol, BS8 1TR, Bristol, United Kingdom

(Received 30 September 2016; accepted 1 December 2016; published online 3 January 2017)

A method for generating stable ultrasonic levitation of physical matter in air using single beams (also known as tractor beams) is demonstrated. The method encodes the required phase modulation in passive unit cells into which the ultrasonic sources are mounted. These unit cells use waveguides such as straight and coiled tubes to act as delay-lines. It is shown that a static tractor beam can be generated using a single electrical driving signal, and a tractor beam with one-dimensional movement along the propagation direction can be created with two signals. Acoustic tractor beams capable of holding millimeter-sized polymer particles of density 1.25 g/cm^3 and fruit-flies (Drosophila) are demonstrated. Based on these design concepts, we show that portable tractor beams can be constructed with simple components that are readily available and easily assembled, enabling applications in industrial contactless manipulation and biophysics. [http://dx.doi.org/10.1063/1.4972407]

Sound is a mechanical wave and as such it carries momentum that can generate acoustic radiation forces.[1–4] When these forces are strong enough and converge from all directions, particles can be levitated against gravity.[5] Acoustic levitation is becoming a fundamental tool in lab-on-a-chip scenarios,[6] microscopy,[7] pharmaceuticals,[8] the levitation of biological samples,[9–11] and even small animals.[12]

Recently, single-beam acoustic levitators have been generated using phased arrays.[13–15] We adopt terminology common in optics and term these single-beams that can trap objects in three dimensions *tractor beams*. Acoustic tractor beams have the potential to revolutionize contactless manipulation due to their high exerted force to input power ratio[15] and the wide variety of supported particle materials as well as sizes. However, phased array systems are currently necessary in order to generate and amplify dozens of independent electric signals making tractor beams not generally accessible due to cost, space, or complexity of operation.

Phased arrays are a collection of elements that emit or receive with specific phases or time delays. They are in widespread use in radar,[16] sonar,[17] and ultrasonic imaging[18] since they can dynamically change the direction or shape of the beam. At present, the phase delays are programmable and achieved using bespoke electronics, but when these systems were first developed the delays were static and introduced with passive elements. For instance, electrical signals were made to travel through long cables to introduce a time delay proportional to its length.[19]

Inspired by these early passive delay lines, we developed devices that modulate a simple wavefront in order to generate an acoustic tractor beam. The sonic devices are composed of several unit cells, and the emitters are mounted into them. Each unit cell introduces a specific phase delay. Our approach parallels developments in 2D planar metamaterials[20–25] where a layer of sub-wavelength unit-cells is used to shape and steer incident fields. In our sonic devices, the phase-shifting unit cells are not limited to the size of the wavelength and the emitters are designed as part of the structure. This approach minimises operational cost and complexity, making tractor beams portable and more readily deployable, hence enabling applications in industrial contactless manipulation and biophysics.

The acoustic pressure P at point $\boldsymbol{r}$ due to a collection of N transducers emitting through a layer of passive delay lines can be written as

$$P(\boldsymbol{r}) = \sum_{n=1}^{N} P_n L_n \frac{D_f(\theta_n)}{d_n} e^{i(\varphi_n + k\Delta_n)}, \tag{1}$$

where P_n is a constant that defines the transducer output power, L_n is a loss factor associated with each delay line, and D_f is a far-field directivity function that depends on the angle θ_n between the effective source normal and $\boldsymbol{r}$. Here, $D_f = 2J_1(ka\sin\theta_n)/ka\sin\theta_n$, the directivity function of a piston source, where J_1 is a first order Bessel function of the first kind and a is the radius of the piston. The term $1/d_n$ accounts for divergence, where d_n is the propagation distance in free space. The phase of the wave at point $\boldsymbol{r}$ is $\varphi_n + k\Delta_n$, where φ_n is the applied electronic phase, Δ_n is the propagation distance between $\boldsymbol{r}$ and the emitters, $k = 2\pi/\lambda$ is the wavenumber, and λ is the wavelength.

It should be noted that the phase of a wave arriving at $\boldsymbol{r}$ can be controlled either by the electronic phase modulation (φ_n) or by the distance that the wave travels (Δ_n). Fig. 1 (Multimedia view) illustrates the three concepts that we used to encode the phases of an electronic phased array into passive sonic devices. In the electronic phased array, the circuitry controls φ_n whereas in the passive devices φ_n is a constant for all the elements and the phase is controlled by changing Δ_n.

Electronic phased array. An electronic phased array in which the elements are all located in a horizontal plane ($z = 0$) is shown in Fig. 1(a). Here, $\Delta_n = d_n = |\boldsymbol{r} - \boldsymbol{s_n}|$ and

[a]Author to whom correspondence should be addressed. Electronic mail: amarzo@hotmail.com.

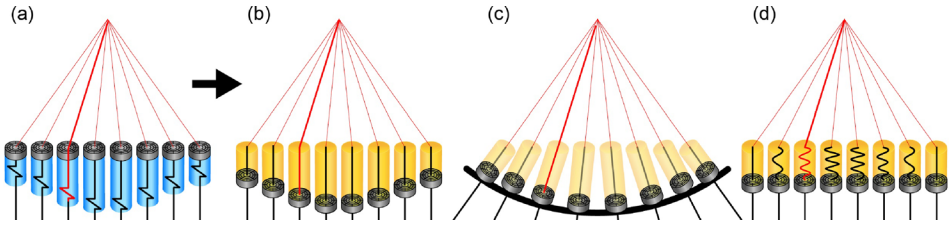

FIG. 1. Focusing a phased array at a target point by electronic delays (a), Straight Tubes (b), Sculpted surface (c), and Coils (d). Notice that the bold red line has the same length for all instances. (Multimedia view) [URL: http://dx.doi.org/10.1063/1.4972407.1]

$\theta_n = Azm\angle(\boldsymbol{r} - \boldsymbol{s_n})$, where $\boldsymbol{s_n}$ is the position of a source and $Azm\angle$ denotes the azimuthal angle. Typically, the element outputs are uniform (i.e., $P_n = P_o$) and there is no insertion loss ($L_n = 1$). For instance, to focus the array at a point $\boldsymbol{f} = (0, 0, f_l)$, the phase modulation is found from simple time reversal as $\varphi_n = k|\boldsymbol{f} - \boldsymbol{s_n}|$.

Straight tubes. In Fig. 1(b), the emitters are attached below vertical rigid tubes of different heights; this sonic device has a flat upper surface. In Eq. (1), $\Delta_n = d_n + h_n$, where d_n is the propagation distance in free space (i.e., once the sound waves have exited the tubes) and h_n is the tube length. If $\boldsymbol{t_n}$ is the position of the tube exit then: $d_n = |\boldsymbol{r} - \boldsymbol{t_n}|$, $\theta_n = Azm\angle(\boldsymbol{r} - \boldsymbol{t_n})$, and $h_n = |\boldsymbol{t_n} - \boldsymbol{s_n}|$. The tube length for introducing a phase modulation of φ is $h = \varphi/k$; this length can be seen as a static alternative to the electronic delay. The tubes have the same diameter as the transducers to facilitate their attachment; wider (or narrower) tubes may cause an increase in the insertion loss and change the linear relation between phase modulation and length.[26] Since continuous wave emission was used, the lengths of the tubes were trimmed according to (h_n modulo λ) where modulo operation gives the remainder of the integer division.

Sculpted surface. The tubes and emitters from the previous device have been aligned with the lines that join the target point and the top of the tubes as illustrated in Fig. 1(c). Therefore, the propagation distance Δ_n remains the same even when the tubes are removed. The emitters are held in place by slots in a shaped surface, which also acts as a supporting structure. In Eq. (1), θ_n and L_n are calculated as in the electronic phased array. The emitters are pointing at the focal point so $\theta_n = 0$ and hence $D_f = 1$, which means that the maximum intensity of the transducers is directed towards the target making this the most efficient possible configuration.

Coils. In Fig. 1(d), the tubes are coiled to fit into a flat rectangular slab. This sonic device was stimulated by the active research in the field of space-coiling metamaterials in which conduits are coiled in different ways.[27,28] In Eq. (1), $\Delta_n = d_n + c_n$, where c_n is the length of the coil, note that the heights of the coils (h_n) are equal and that c_n depends on the coil revolutions. Since the coiling requires extra space inside the unit cell, the coil diameter is reduced in the inner region. We used horns[29] at the entrance and exit of the coil to transition between the diameter at the entrance and exit (transducer diameter) and the inner reduced diameter. The model for the coil follows closely that of the tube for d_n and θ_n.

An acoustic tractor beam is generated by focusing the array at a target position and then adding a static phase signature that only depends on the type of trap to be generated; three distinct phase signatures have been shown to generate functional tractor beams.[14] Briefly, if half the array is excited out-of-phase, then a Twin trap results; if a central circular aperture is driven out-of-phase, then a Bottle trap is generated; and if a helical phase ramp is used, then a Vortex trap results. We focused our designs on the Twin trap since the Vortex trap can only seize small particles without ejecting them and the Bottle trap has relatively weak lateral forces.[14] However, it should be noted that the presented devices could easily be altered to generate any type of trap.

To excite the out-of-phase elements needed for a Twin trap there are two options: introducing the π-phase offset in the delay lines by lengthening or shortening them by a distance of $\lambda/2$ or by reversing the polarity of the emitters. Introducing the signatures directly to the delay lines creates an integrated simpler structure but introduces small dissimilarities in the attenuation per element as different length tubes or coils are required. Switching the polarity requires a specific cable-transducer attachment and so is not such a flexible solution, but it leads to simple and more uniform surfaces. For the Straight tubes and Coils, we used the former method whereas for the Sculpted surface we used the latter leading to a simpler surface with all the emitters having the same distance to the target.

For the practical realization of the devices, we used transducers operating at 40 kHz ($\lambda = 8.5$ mm): 10 mm diameter transducers (MA40S4S) for the Straight Tubes and Coils, and 16 mm diameter transducers for the Sculpted Surface (MCUSD16P40B12RO). With this configuration, the Straight tubes had a directivity (D_f) similar to that of the piston source (see supplementary Figs. 1 and 2), the linear relation ($h = \varphi/k$) was found to hold ($R^2 = 0.997$) (see supplementary Fig. 3), and the loss factor was $L_n = 0.8$ on average (see supplementary Fig. 4). For the coils, the relation between coil revolutions and phase modulation is presented in supplementary Fig. 5. The coils were 10 mm diameter at the entrance and exit and 2 mm in the inner region; this configuration reduced the insertion loss (see supplementary Fig. 6). The coil horns produced a directivity function similar to a piston source (see supplementary Figs. 1 and 2). The insertion loss for the coils depending on the revolutions and on average was $L_n = 0.7$ (see supplementary Fig. 7). The devices developed to create a Twin trap using a single driving signal are illustrated in Fig. 2 (Multimedia view). These devices are portable as well as created with components that can be bought and put together by anyone (A step by step video is included in the supplementary material, and the source code and 3D files can be found online).

When the three passive devices are powered with a single driving signal, they generate a tractor beam. In Figs. 3(a)–3(d) (Multimedia view), we show the modelled and experimental acoustic pressure amplitude (see supplementary material) for a Twin trap generated with a Coil device. Figs. 3(e)–3(h)

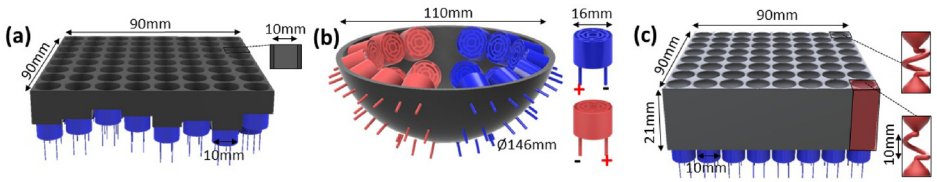

FIG. 2. Realization of sonic devices for generation of tractor beams with a single driving signal. (a) Straight Tubes with 8 × 8 delay lines and transducers attached below; the tube length varies between 5 mm and 14 mm to provide the phase modulation. (b) Sculpted Surface with three rows of 14 (top), 10 (middle), and 6 (bottom) transducers, 30 in total. (c) Coils with 8 × 8 delay lines. (Multimedia view) [URL: http://dx.doi.org/10.1063/1.4972407.2]

show a Vortex trap generated with a Straight tubes device. The agreement between experiment and prediction is good, especially around the trapping point. Also, full three-dimensional Finite-Difference Time-Domain (FDTD) simulations were performed and found to be in good agreement with the simple model expressed by Eq. (1) (see supplementary Fig. 8).

The three devices were able to levitate expanded polystyrene (EPS) spheres of $R_p = 2$ mm, which given a density $\rho_{EPS} = 29\,\mathrm{kg/m^3}$ represents a levitation force of 1 μN. The size limit is imposed as the devices levitate in the Rayleigh scattering regime in which the particle has to be small in comparison to the wavelength. The EPS particles were levitated vertically (i.e., above an array located in the x-y plane) and laterally (i.e., to the side of an array located in the x-z plane); in the case of the Sculpted surface devices also levitation upside down was achieved (i.e., below an array located in the x-y plane). Additionally, it was possible to levitate a particle of polymer (Polylactic Acid, $\rho_{PLA} = 1250\,\mathrm{kg/m^3}$, dia. 1.85 mm, thickness 0.5 mm) as well as fruit-flies (Drosophila, 0.3 mg each). A collection of these scenarios is shown in Fig. 4 (Multimedia view).

Device performance was measured experimentally by levitating a $R_p = 1$ mm EPS sphere with a Twin trap 1.8 cm above the surface and finding the minimum required voltage. This ranked the Sculpted surface as the most effective device, followed by the Straight tubes and then the Coil device. In brief, a drive signal of 14Vpp (5.6 W) was required for levitation using the Sculpted surface, 34Vpp (27.2 W) for the Straight tubes, and 43Vpp (51.6 W) for the Coils. In the normal regime of operation, the pressure generated by an emitter is proportional to the voltage of the driving signal. The trapping stiffness is the Laplacian of the Gor'kov Potential,[14] which is proportional to the square of the pressure. Therefore, the trapping stiffness generated by our devices can be expressed as $K = \varepsilon V^2$, where ϵ is a coefficient that defines the device efficiency and V is the applied voltage. The ε was 2.35 for the sculpted surface, 0.39 for the Straight tubes, and 0.24 for the Coils. These differences can be explained by the relatively high loss factors of the Coils (on average $L_n = 0.7$) and because the flat arrangement of transducers incurs losses due to directivity effects (i.e., the transducers are not directed to the focal point). Good agreement was found with Eq. (1) (RMSD = 0.06), which gave

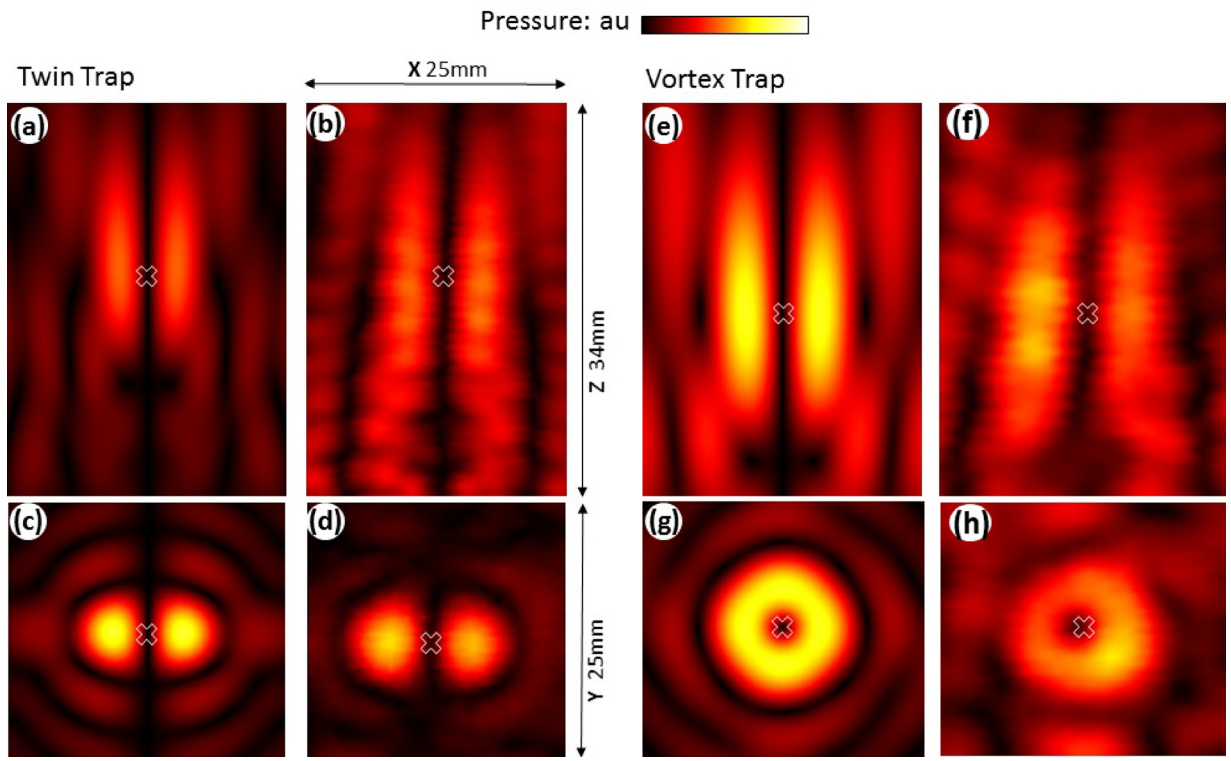

FIG. 3. Amplitude of the acoustic field in simulations (a), (c), (e), and (g) and experiments (b), (d), (f), and (h). For a Twin trap generated with a Coil device 2.5 cm above the surface (a)–(d); and a Vortex trap generated with a Straight tube device (e)–(h). Z is the direction of beam propagation and X-Y is the transversal plane. The trapping point (marked with an X) was at 2.5 cm height from the top center of the devices. (Multimedia view) [URL: http://dx.doi.org/10.1063/1.4972407.3]

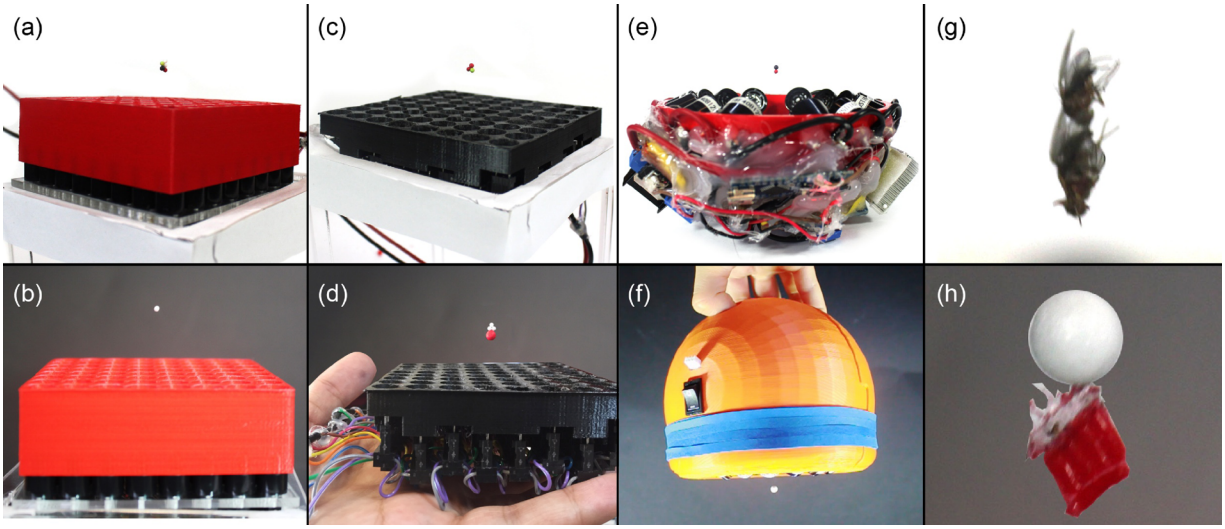

FIG. 4. Different particles levitated in the three sonic devices. (a) and (b) Coil device, (c) and (d) Straight tube device, and (e)–(h) Sculpted surface device. (a) Four Rp = 1 mm EPS beads levitating 1.8 cm above a Coil device and (b) a single one levitating 2.5 cm above. (c) Three Rp = 1 mm beads levitated in a Straight tube device and (d) a Rp = 2 mm bead with three Rp = 1 mm on top. (e) Sculpted surface device levitating two Rp = 1 mm beads, (f) Rp = 2 mm bead upside down, (g) two fruit-flies levitated vertically, and (h) PLA particle levitating below an Rp = 2 mm EPS bead. (Multimedia view) [URL: http://dx.doi.org/10.1063/1.4972407.4]

predicted stiffness coefficients of $\varepsilon = 2.25$, 0.39 and 0.31, respectively.

The three devices were excited using a single electrical drive signal and consequently they produced a static trap. However, it is possible to exploit geometric symmetries to achieve dynamic focusing of the trap using a reduced number of signals. We first note that in an axisymmetric arrangement the distance between any point on the revolution axis and the transducers in a given row is the same; therefore, a single signal can be used to drive all the transducers in that row, swapping the polarity in the opposite half of that row to get a Twin trap. We then achieve dynamic trapping by following the technique used in concentric-ring phased arrays to refocus the beam at different heights.[30] We used the Sculpted Surface device presented in Fig. 2(b) with the bottom row of transducers removed, leaving only the top and middle rows; the electronic circuit is presented in supplementary Fig. 9 and the arrangement in supplementary Fig. 10. To explore the functionality of this two channel arrangement, the particle was placed in the natural focus of the bowl (1.8 cm above the top) and the relative phase of the two 25Vpp excitation signals was changed to move the particle upwards in increments of 0.5 mm until the particle fell out of the trap under gravity. With this setup, the maximum height reached with an EPS bead Rp = 1 mm was 4.5 cm above the top of the spherical cap. Axisymmetric designs of the other sonic device concepts would enable them to use this feature.

Three types of passive devices capable of generating acoustic tractor beams have been demonstrated. They employ a small number of electric driving signals, making them a significant simplification over existing tractor beams which require electronic phased arrays with dozens of independent signals. The Sculpted surface sonic device is the most efficient device but Straight tubes and Coils have the advantage of presenting a flat emitting surface, making them more widely deployable. Additionally, Coil devices could use a single source since they are also flat on the lower surface. The ability of phased arrays to steer the beam has been replaced here in favour of a more portable, affordable, simple, and compact solution. This trade-off is desirable for scenarios that require levitation at fixed locations (which could potentially be coupled with mechanical motion) or limited movement with the addition of a small number of independent channels. The presented sonic devices have the potential to make acoustic tractor beams a widespread solution in contactless manipulation.

See supplementary material for information about the construction of the sonic devices, the driver board, as well as the simulated and experimental fields. It also contains experimental measures and model fits for the directivity of each delay line (supplementary Figures 1 and 2), phase modulation for the tubes (3), insertion loss of tubes (4), phase modulation for different coil revolutions (5), attenuation of different horns (6), insertion loss for different coil revolutions (7), FDTD simulations (8), Electronic circuit (9), and dynamic refocusing (10). The clip "Dynamic Trap" shows a simulation of the trap being refocused dynamically using 2 channels. The clip "Step by Step assembly" shows how to assemble a portable tractor beam step by step.

This project has been funded by the UK Engineering and Physical Science Research Council (EP/N014197/1). We thank Matt Sutton for assisting with the elaboration of both figures and videos contained in this paper. All the data needed to reproduce the results are contained within the paper.

[1]L. V. King, Proc. R. Soc. London **147**(861), 212 (1934).
[2]L. P. Gor'Kov, Sov. Phys. Doklady **6**, 773 (1962).
[3]A. A. Doinikov, J. Acous. Soc. Am. **100**(2), 1231 (1996).
[4]H. Bruus, Lab Chip **12**(6), 1014 (2012).
[5]E. H. Brandt, Nature **413**(6855), 474 (2001).
[6]X. Ding, S. C. S. Lin, B. Kiraly, H. Yue, S. Li, I. K. Chiang, and T. J. Huang, Proc. Natl. Acad. Sci. **109**(28), 11105 (2012).
[7]H. M. Hertz, J. Appl. Phys. **78**(8), 4845 (1995).

[8]R. J. Weber, C. J. Benmore, S. K. Tumber, A. N. Tailor, C. A. Rey, L. S., Taylor, and S. R. Byrn, Eur. Biophys. J. **41**(4), 397 (2012).
[9]L. Puskar, R. Tuckermann, T. Frosch, J. Popp, V. Ly, D. McNaughton, and B. R. Wood, Lab Chip **7**(9), 1125 (2007).
[10]T. Vasileiou, D. Foresti, A. Bayram, D. Poulikakos, and A. Ferrari, Sci. Rep. **6**, 20023 (2016).
[11]M. Sundvik, H. J. Nieminen, A. Salmi, P. Panula, and E. Hæggström, Sci. Rep. **5**, 13596 (2015).
[12]W. J. Xie, C. D. Cao, Y. J. Lü, Z. Y. Hong, and B. Wei, Appl. Phys. Lett. **89**(21), 214102 (2006).
[13]C. E. Démoré, P. M. Dahl, Z. Yang, P. Glynne-Jones, A. Melzer, S. Cochran, and G. C. Spalding, Phys. Rev. Lett. **112**(17), 174302 (2014).
[14]A. Marzo, S. A. Seah, B. W. Drinkwater, D. R. Sahoo, B. Long, and S. Subramanian, Nat. Commun. **6**, 8661 (2015).
[15]D. Baresch, J. L. Thomas, and R. Marchiano, Phys. Rev. Lett. **116**(2), 024301 (2016).
[16]A. J. Fenn, D. H. Temme, W. P. Delaney, and W. E. Courtney, Lincoln Lab. J. **12**(2), 321 (2000).
[17]J. H. G. Ender and A. R. Brenner, IEEE Proc.-Radar, Sonar Navig. **150**(3), 165 (2003).
[18]B. W. Drinkwater and P. D. Wilcox, NDT&E Int. **39**(7), 525 (2006).
[19]T. L. Gereld, U.S. patent 2,387,783 (30 October 1945).
[20]Z. Liang and J. Li, Phys. Rev. Lett. **108**(11), 114301 (2012).
[21]Y. Li, B. Liang, Z. M. Gu, X. Y. Zou, and J. C. Cheng, Sci. Rep. **3**, 2546 (2013).
[22]Y. Li, X. Jiang, R. Q. Li, B. Liang, X. Y. Zou, L. L. Yin, and J. C. Cheng, Phys. Rev. Appl. **2**(6), 064002 (2014).
[23]Y. Li, X. Jiang, B. Liang, J. C. Cheng, and L. Zhang, Phys. Rev. Appl. **4**(2), 024003 (2015).
[24]K. Tang, C. Qiu, J. Lu, M. Ke, and Z. Liu, J. Appl. Phys. **117**(2), 024503 (2015).
[25]X. Jiang, Y. Li, B. Liang, J. C. Cheng, and L. Zhang, Phys. Rev. Lett. **117**(3), 034301 (2016).
[26]H. Tijdeman, J. Sound Vib. **39**(1), 1 (1975).
[27]Y. Xie, W. Wang, H. Chen, A. Konneker, B. I. Popa, and S. A. Cummer, Nat. Commun. **5**, 5553 (2014).
[28]X. Zhu, K. Li, P. Zhang, J. Zhu, J. Zhang, C. Tian, and S. Liu, Nat. Commun. **7**, 11731 (2016).
[29]E. Bängtsson, D. Noreland, and M. Berggren, Comput. Methods Appl. Mech. Eng. **192**(11), 1533 (2003).
[30]C. A. Cain and S. I. Umemura, IEEE Trans. Microwave Theory Tech. **34**(5), 542 (1986).